15 KHz Active Sonar System with Linear Beamforming Microphone Array

Helmuth Naumer and Mark Theng

May 17, 2018

Abstract

We designed and built a 5V 15 KHz active sonar system with a linear array of three microphones. Using a linear array of 3 omnidirectional microphones and one speaker, we broadcast a brief 15 KHz tone and time the return to estimate distance. By driving the microphones out of phase, we selectively amplify signals coming from a given angle. A reading is obtained when the peak signal magnitude rises above a specified threshold. The results are displayed on an oscilloscope in the form of a small circle drawn wherever an object is detected. On the display, the y axis corresponds to angle and the x axis corresponds to distance.

1 Introduction

Directional range finding systems are more than just a cool technology: they've found applications in everything from environmental science mapping oceans [1] to defense. While it's possible to design a complicated antenna or microphone to be highly directional, and then move it mechanically, it's often preferred instead to simply maintain an array of inputs and/or outputs. By looking at the path length difference of the wave and carefully applying different phase shifts to each input, we can steer the transmitting and/or receiving beams into the right direction. Figure 2 provides a visual of the important parameters for linear array beamforming.

While recent developments in beamforming such as attempts to exploit multipath propagation [2] would be almost impossible to implement in analog, and completely infeasible in the timeline of a couple of weeks on a breadboard, it's still possible to create a small, simple system that demonstrates this incredible application of interference strongly enough for an interesting demonstration of the concept.

2 System Design

The system design process began with a careful consideration of the signal processing concepts to set initial goals within the architecture. In the final result, you can see that the greatest failures in the performance of the final system are from the positions where the signal architecture specs weren't met.

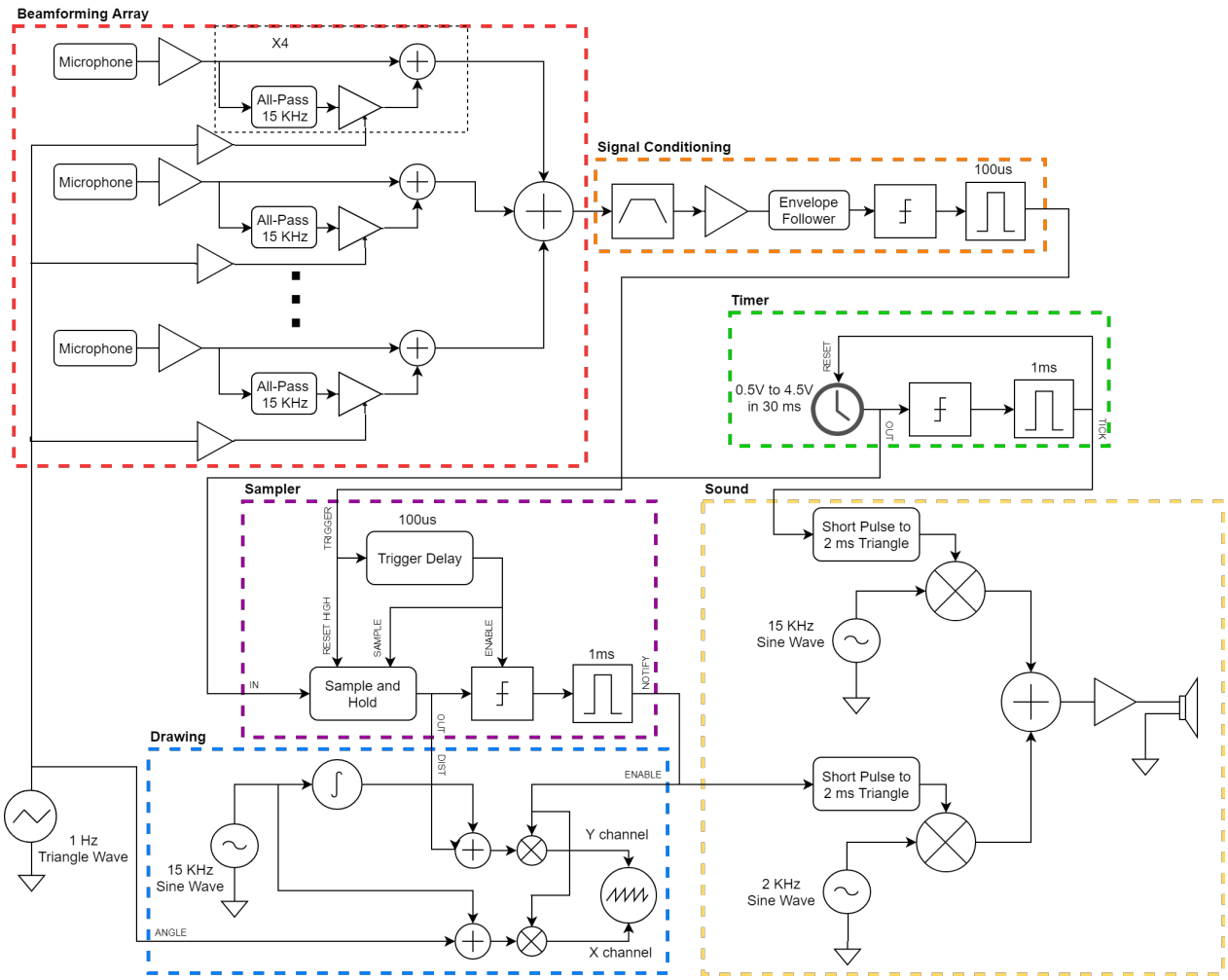

Figure 1: Complete Block Diagram

2.1 Overall Design

Many architectural design decisions were required for the successful implementation of the system. Due to the interface with the real world, potential interference and physical limitations took a larger role. While the architectural design decisions will be described in more detail within the relevant subsections, a brief overview of some of the major decisions is provided here.

Choosing to work with sonar allowed our project to be a lot simpler than radar, not just because of the significantly lower frequencies involved, but also because the speed of sound is a lot slower than the speed of light. The large time between the transmission and reception of the audio pulse allows us to measure this return time with a simple thresholding and timer circuit, instead of using more complicated techniques like pulse compression.

The 15 KHz frequency of the pulses was chosen for a few reasons. The first reason was to hopefully make it a little robust to ambient noise in the room, but was we ultimately discovered that this did not help as much as we had hoped. Another reason was to allow for shorter pulses. As the frequency is lowered, the central lobe takes up a high percentage of the frequency band, potentially even acquiring a significant DC offset component in extreme cases. These shorter pulses also have the benefit of providing a greater distance resolution. 15

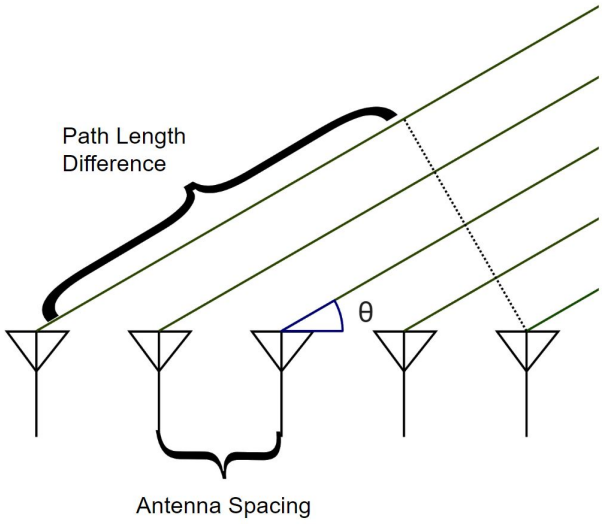

Figure 2: Beamforming Array Principles

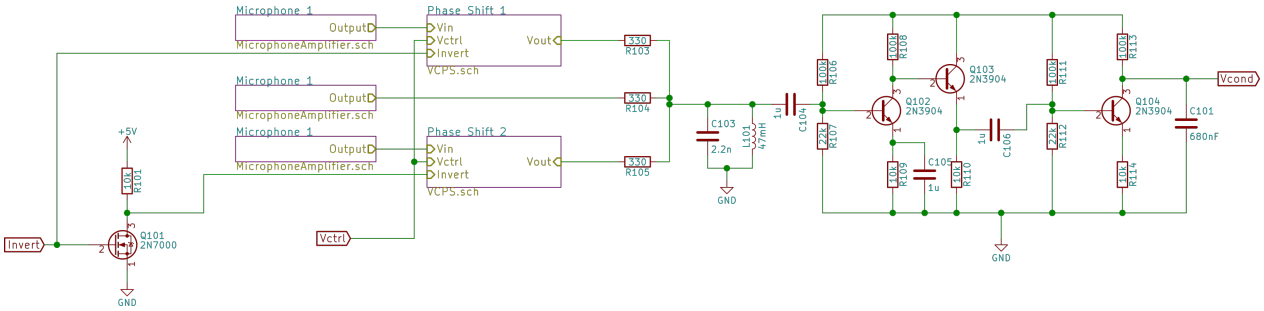

Figure 3: Beamforming Circuitry

khz was also low enough for regular speakers and microphones, rather than more specialized devices. Finally, the geometry of our array is determined by frequency. With 15 15Khz, the microphones only needed to be spaced slightly more than 1 cm apart.

The overall design of our circuit evolved considerably over the initial few weeks of our project. We had initially planned to shift the direction of beamforming and send out a new audio pulse immediately when a signal is detected by the microphones. We eventually eliminated those feedback loops in our final design by generating the beamforming direction and audio pulses independently of the detection of return signals. The simplicity of this linear design more than compensated for any slight decreases in speed we had by forgoing the more controlled approach.

2.2 Beamforming Array

***Designer*: Helmuth Naumer**
Inputs: 15 KHz Sound Pulse
Outputs: Beamformed audio signal (0V-5V possible)

2.2.1 Overview

Linear array beamforming focuses the antenna array though applying phase shifts to the inputs of each antenna. By looking at the geometry of the array, we can derive a path length difference for the wave to travel. See figure 2 for a visual of the claim. This path length difference is equivalent to sampling the wave at different points discretely, and can be interpreted as applying a phase shift to the wave that is dependent on angle. By adding the signals together, they can either constructively or destructively interfere with each other creating a focused beam in a desired direction.

We can easily derive the path length difference, δ, based on the geometry of the array. Denote the spacing between receivers to be l, the angle off the center to be θ, and assume that we are receiving a plane wave coming sufficiently far from the receivers. By looking at the right triangle formed by placing a line orthogonal to the direction of propagation of the wave, we can compute the difference to be $nl\cos(\theta)$, where n denotes the number of elements away. By carefully placing the elements of the array at $\frac{\lambda}{2}$ steps, we can see that this can be written as $\frac{n\lambda\cos(\theta)}{2}$, and as a fraction of λ, provides a phase shift of $\frac{n\lambda\cos(\theta)2\pi}{2\lambda} = \pi n\cos(\theta)$. Finally, if we are only looking for perturbations off of the central axis, this can further be simplified to a phase shift of $\phi = n\pi\theta$ by the small angle approximation.

We then need to compute how the phase shift impacts the final output of the microphone. Consider first a setup with only two microphones in which the two microphones have opposite phase shifts applied to them. We will denote the phase shift applied by the voltage controlled phase shifting system to be Φ, while the phase shift from the path length difference will be ϕ.

To abbreviate the analysis for this report, we will demonstrate only that the central lobe is indeed at 0 when the two are signals are summed together. By applying the phase shifts from the path length difference, we compute that the two microphones receive the signals $\cos(2\pi ft)$ and $\cos(2\pi ft+\phi)$. After applying the system's controlled phase shift and summing the results, we have:

$$\cos(2\pi ft + \Phi) + \cos(2\pi ft + \phi - \Phi) = \cos(2\pi ft + \Phi) + \cos(2\pi ft + n\pi\theta - \Phi)$$

$$\cos(2\pi ft + \Phi) + \cos(2\pi ft + n\pi\theta - \Phi) = \cos(2\pi ft)(e^{j\Phi} + e^{-j(\Phi+n\pi\theta)})$$

We can see easily that the signal amplitude is now independent of the beamforming amplitude, and that we must simply look for maximums and minimums in the expression $(e^{j\Phi} + e^{-j(\Phi+n\pi\theta)})$. If we further split $n\pi\theta$, we can get further simplify the expression, and provide something more easily to analyze.

To speed the analysis, simulations for many parameters beyond these were completed in a Julia notebook.

Each microphone is initially be amplified to help keep it more robust to signals picked up in the circuit or noise from the devices. Following the amplifier, the signal will split into two paths. On one path there will be an all pass filter tuned to provide a 90 degree phase shift at 15 Khz. Because so much depends on the pole being placed reliably, an op amp configuration will be used. Finally, we'll have a voltage controlled BJT amplifier. By summing the two paths together, we can produce a voltage controlled phase shift up to 90 degrees. In order to reach greater phase shifts than possible with one block of the circuit, we cascaded multiple voltage controlled phase shifters to get the desired affect.

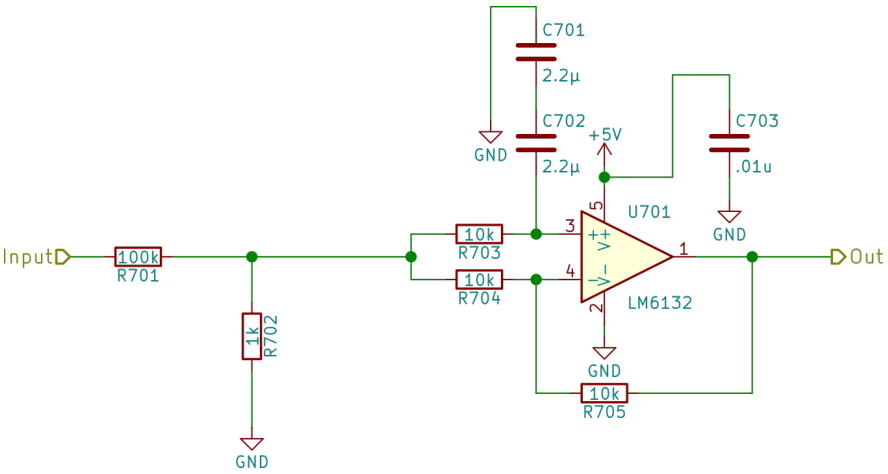

Figure 4: Standard Op-Amp All Pass Filter Topology

The signals were buffered before the summing to ensure that the previous stages weren't impacted by the output resistance

2.2.2 Circuits

The circuit is comprised primarily of simple 10X gain stages, all pass filters, and a voltage controlled amplifier.

All Pass Filter:

Figure 4 shows an all pass filter topology which applies a phase shift of $\Delta\theta = 2\tan^{-1}(1/(\omega RC))$ [3]. The circuit has a transfer function of $H(s) = \frac{s-\tau}{s+\tau}$. By placing pole and zero reflected across the imaginary axis, we effectively minimize the impact of gain in the circuit, and simply provide a phase shift.

Voltage Controlled Amplifier:

Figure 5 shows the voltage controlled amplifier topology used in this design. By varying V_{ctrl}, we are able to tune the gain in the stage by changing the quiescent current in the Q1. The small signal voltage gain in a standard common emitter stage can be expressed as $a_v = \frac{I_c R_L}{V_{th}}$

Audio Amplifier:

Figure 6 shows the audio amplifier topology used. It is a very simple design which uses two gain stages and two buffers. Because of the low output impedance of the microphone and the degeneration of the gain stages, we opted not to include a buffer after the raw microphone output. It may have been possible to remove the first buffer stage as well to limit components, but it was included as a precaution.

The input impedance into the gain stages can be approximated by impedance reflection. By choosing a conservative value of $\beta \approx 100$, we can approximate the input impedance of each gain stage to be $(10k\Omega)\beta \approx 1M\Omega$. While this degeneration provides much greater input resistance, we lose the gain down to only $\frac{R_L}{R_{deg}} = 10$ for each stage, and thus cascade two to get an overall gain of 100.

Phase Splitter:

In order provide phase shifts in both directions, we use the phase splitter circuit seen in figure 5. This circuit is almost a combination of a common emitter and emitter follower. While each output provide roughly a magnitude gain of 1, the upper output inverts. By

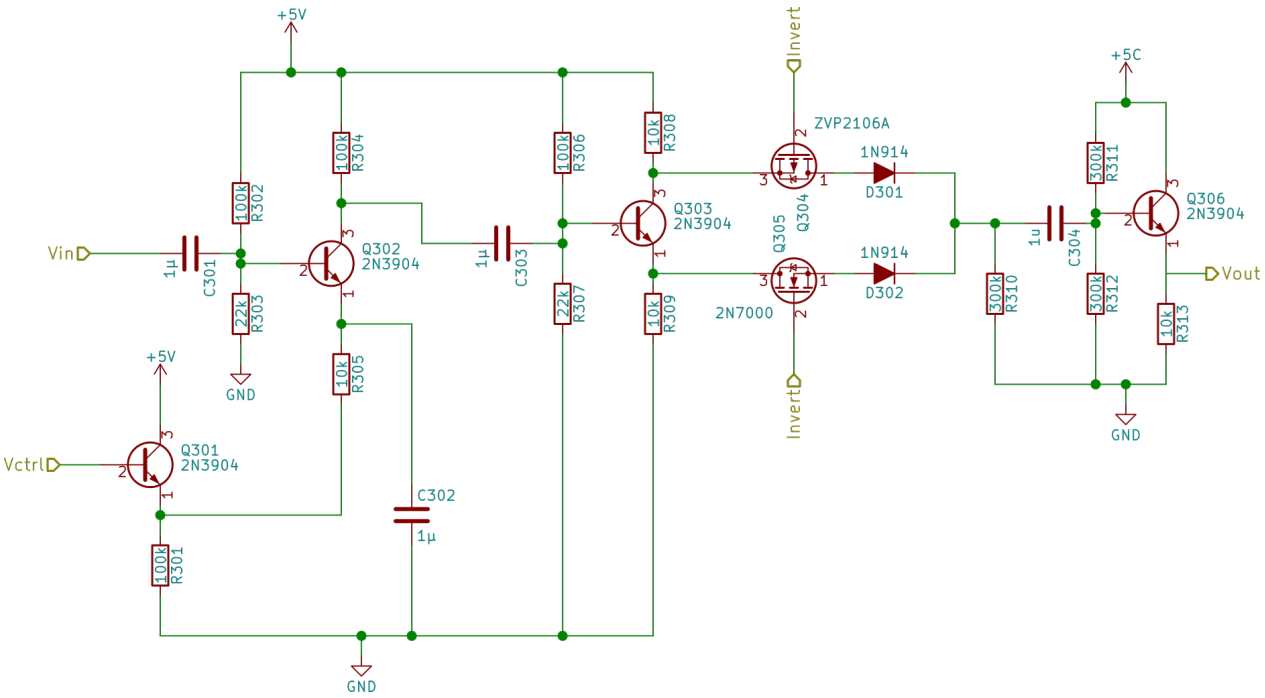

Figure 5: Voltage Controlled Amplifier, Phase Splitter, Unidirectional Analog Multiplexer, and Buffer

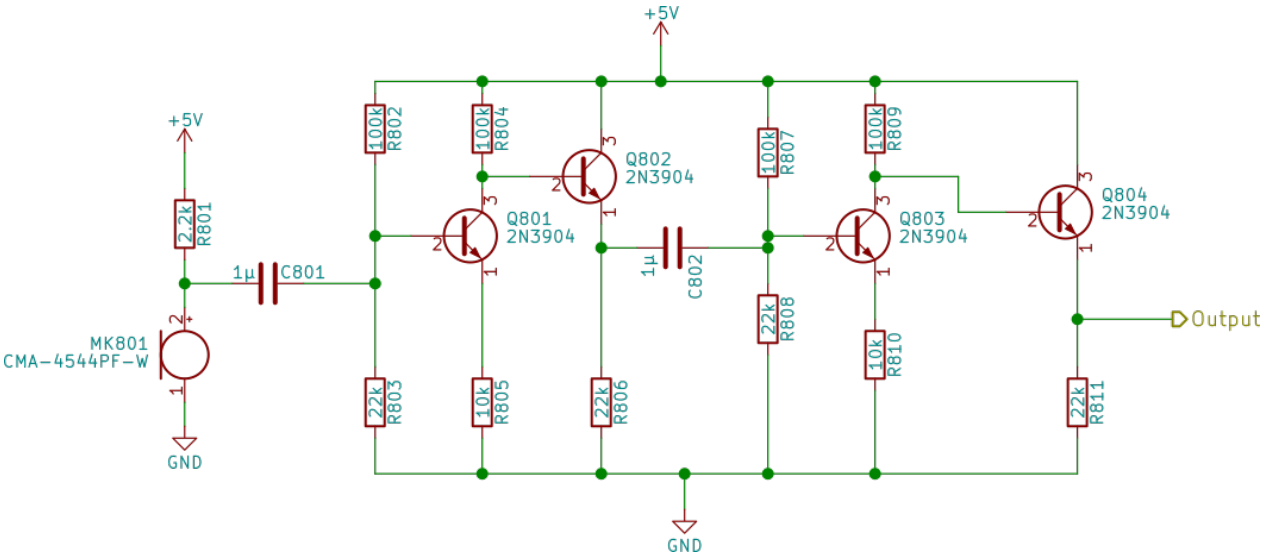

Figure 6: Audio Amplifier

cascading this circuit with our all pass filters, we're able to provide phase shifts in both directions.

Analog Multiplexer:

Finally, in order to choose between the two possible outputs, we have a simple analog multiplexer comprised of two mosfets and a pair of diodes which can be seen in figure 5. By sending a control signal, one of the two mosfets begins to conduct, allowing us to choose either the inverting or non-inverting output of the phase splitter.

2.2.3 Testing

Initially, as each block was built, it was tested using a function generator set to 15 kHz and an oscilloscope to ensure that the correct behavior is occurring. Once each sub-block was working correctly, the complete system was tested by using a mobile speaker playing a tone of 15 kHz. The speaker was moved around the setup while the output is probed to observe the directionality of the array. A separate constant control signal was provided to the phase shifters, and the sweep was done again.

2.2.4 Results

While our original design and simulations was for an array with 7 elements, our final result included only three. While out performance was lower, it still acted as a proof of concept which correctly aligned with the theory and simulations for the more limited array. Figure 7 shows simulations of two different setups. The left simulation demonstrates the goal set by the initial signal architecture of using 7 microphones with a Bartlett window, while the right simulation represents the setup that we had in the end, using only three microphones using only a rectangular window. Our architecture was adapted to remove the Bartlett window once the number of elements in the array became limited to preserve a more narrow central lobe at the expense of larger sidelobes.

In our experiments, the reflecting object had to be fairly far from the targeted direction to be ignored, which aligns correctly with the simulations. In addition, if the amplitude of the signal was great enough, it could still be picked by by the first large sidelobe which can be seen reflected across the central axis.

The circuits appeared to meet the signals theory.

2.3 Signal Conditioning

***Designer*: Helmuth Naumer**
Inputs: Beamformed audio signal (0V-5V possible)
Outputs: Conditioned signal

2.3.1 Overview

After the array, the signal needs to go through multiple additional blocks of processing. We first band-pass filter the signal with a passive high Q circuit to eliminate other sounds that we may be picking up. The signal is then amplified one final time by a 3-BJT amplifier before going into a circuit that thresholds it based on its envelope. The envelope follower is comprised of a diode, capacitor and resistor for tuning the discharge rate. If above the threshold, a short trigger signal is sent to the timing circuitry.

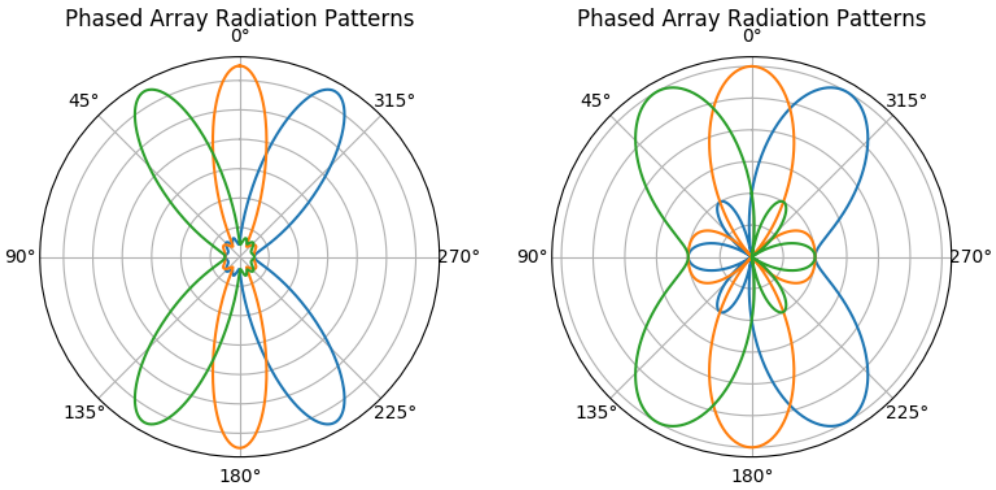

Figure 7: Simulated Radiation Patterns. Left: Designed radiation pattern with 7 microphones. Right: Resulting microphone array simulated radiation pattern. Note also the change in scale radially.

2.3.2 Circuits

The first few stages of amplification is shown in Fig. 3. This includes the LC tank bandpass filter, and the 3-BJT amplifier. The envelope follower is shown in 9.

Bandpass filter

The bandpass filter was simply an RLC circuit. The resistance was controlled by the output resistance of the previous averaging circuit. Because inductors are a more rare commodity in lab, we chose $L = 47mH$ due to its inclusion in the 6.002/6.003 labkit. The capacitor value was chosen to place the resonance at $\frac{1}{2\pi\sqrt{LC}} \approx 15kHz$. $C = 2.2nF$ was the closest option, which sets the resonant frequency to be $15.6kHz$.

Audio Amplifier

The audio amplifier includes a high gain stage, a buffer, and moderate gain stage. The first gain stage is a common emitter amplifier with a degenerative resistor to stabilize the bias point, and a moderate capacitor to recover the high AC gain. Following this stage, there is an emitter follower buffer and a final 10X common emitter stage.

Envelope Follower

The envelope follower is similar to the one built in a previous lab. Using a diode going into a parallel connection of a capacitor and resistor, the capacitor is charged. The capacitor constantly discharges slowly through the resistor, thus following the peaks of the signal.

2.3.3 Testing

Each block was initially tested separately. We swept the frequency for the band pass filter to characterize the bandwidth. We then sent a 15 KHz signal through the amplifier and measured the gain. We sent an AM modulated 15 KHz signal through the full circuit to test the full subsystem.

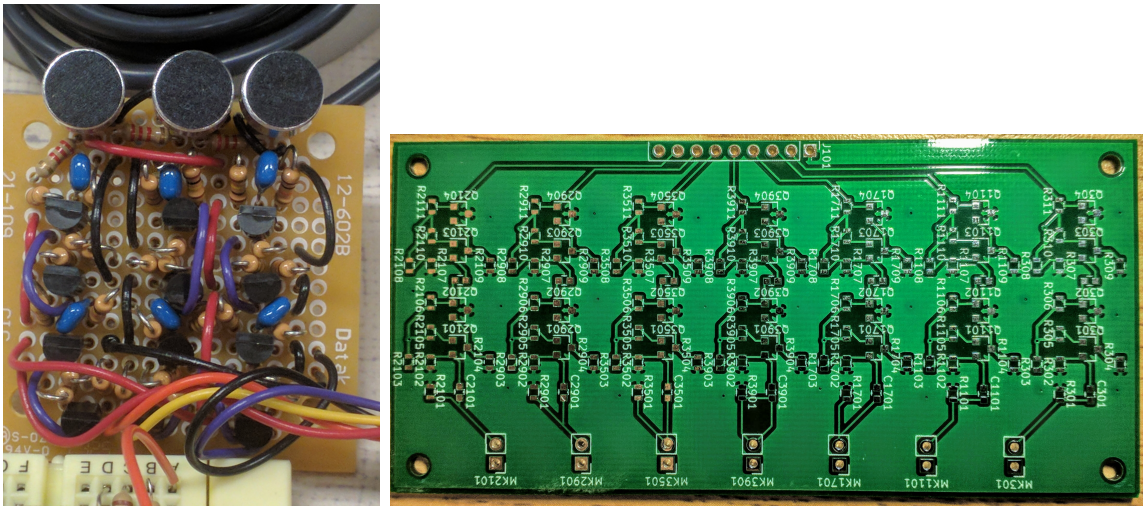

Figure 8: Photos of Microphone Array and Unpopulated PCB

2.3.4 Results

Due to part variations, the RLC bandpass filter was centered at 16.5 kHz, rather than at 15 kHz. Because of this, the resistors had to be modified to allow it to contain the 15 kHz pulse, and resulted in much wider bandwidth than anticipated initially. Thus, more precise parts would help to improve the robustness of our system to speech and other surrounding projects.

Other components worked as designed, but modifications had to be made during the integration of the system due to unexpected interference from the power rails. While adding more capacitors to the power rails certainly helped, the slight perturbations could still be amplified by 1000 going through the circuit and result in incorrect readings and seemingly noisy signals.

2.4 Signal Thresholding

***Designer*: Mark Theng**
Inputs: TICK (1ms >4.5V trigger every 6ms), Conditioned signal
Outputs: Thresholded pulses (>100us 5V)

2.4.1 Overview

The signal thresholding module is responsible for producing clean pulses to indicate to the control circuitry that an echo has been detected. Since many parameters of this module depend on the physical setup and environment of the project (such as the strength of the signal and interference from other sources), most of this module was designed on-the-fly and would likely differ considerably in other implementations of this project. The main components of this module are a variable amplifier, a thresholding circuit, and a pulse extender and AND gate to mask out the initial false signal due to the direct path from the speaker to the microphones.

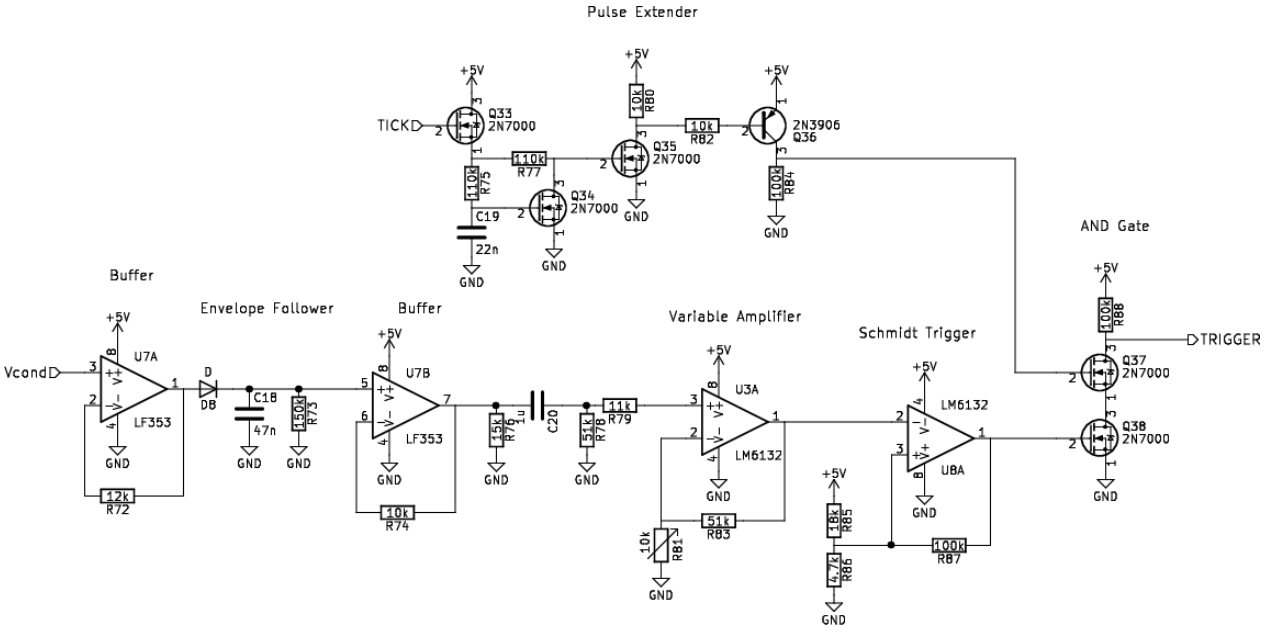

Figure 9: Signal thresholding circuit

2.4.2 Circuit Insights

Since the envelope follower is very sensitive to its output resistance, a buffer is necessary to isolate it from the rest of the thresholding circuitry. Since the signal from the envelope follower is rectified, this signal is AC-coupled to ground (using C20 in Fig. 9) to provide room for subsequent amplification.

The variable amplifier amplifies the envelope follower's output by at least 6 times. This is necessary because the signal from the envelope follower is very small. The signal is then fed into a Schmidt trigger for thresholding. For ease of testing and configuration, a variable resistor is used in the amplification stage to allow us to tune the threshold.

A Schmidt trigger is used here because the signal is expected to be very noisy. This minimizes unnecessary oscillations in later parts of the circuit that could contribute to power supply noise.

Finally, the TICK pulse from the timer is used to mask out the initial speaker pulse. A pulse extender similar to the one used in the timer module (we go into further detail about the pulse extender in that section) is used to extend the length mask to account for the time taken for the sound emitted by the speaker to travel to the microphones. As seen in Fig. 20, only signals sufficiently far away in time from the initial speaker pulse are registered as readings.

2.5 Sound Pulse

***Designer*: Helmuth Naumer**

Inputs: Trigger Signal

Outputs: Audio Pulse

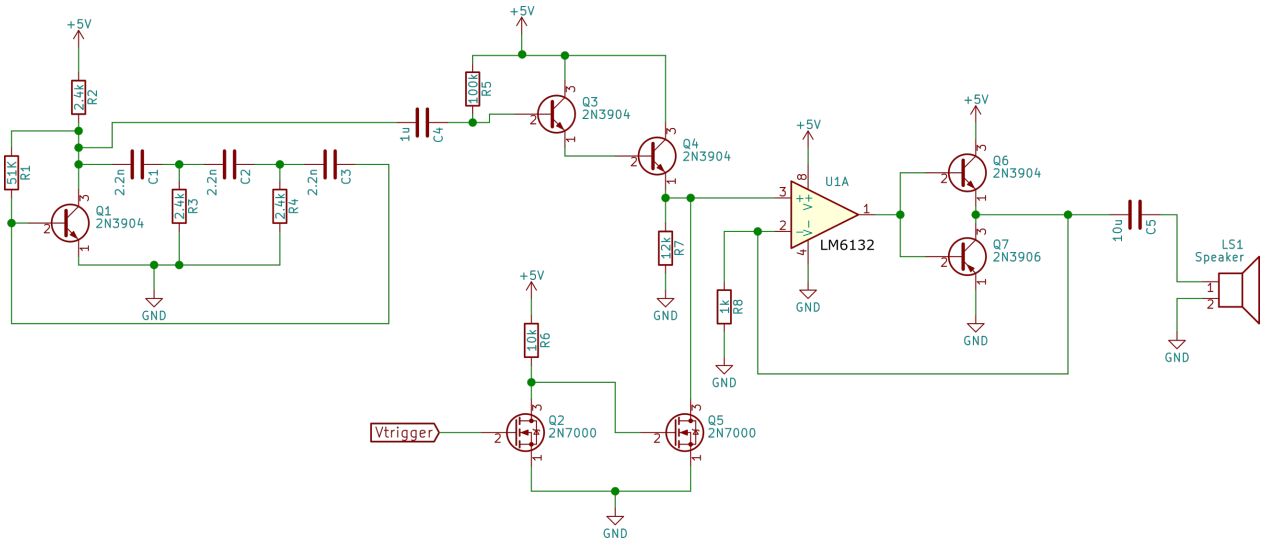

Figure 10: Speaker Circuits

2.5.1 Overview

In order to actually transmit the pulses, we needed to have a simple audio output amplifier. It was designed to operate with a coin sized, 0.3W speaker, and thus only needed to be able to provide at most under 200 mA of current, which is within the specifications of a standard 2N3904 transistor.

2.5.2 Circuits

The power amplifier was simply a voltage buffer using an op-amp and a push-pull bjt output stage. The opamp limits the crossover distortion in the output.

In order to pulse the output, we simply inverted the trigger signal and use the inverting signal to pull the op amp input to ground.

The oscillation was created using a phase shift oscillator with parts selected to oscillate at just over 15 KHz. The darlington pair was vestigial from a previous test that required a lower DC voltage.

2.5.3 Results

In the end, the speaker simply sent out short rectangular pulses of 15 KHz. We had intended to put a bartlett window using the same voltage controlled amplifier as other sections of the project, but simply didn't have time to assemble another one. The intended design was to simply integrate the trigger signal and send it to V_{ctrl} of the amplifier to mix the two signals.

Due to the level of volume from the small omnidirectional speaker, many tests were performed with an old desktop speaker instead.

2.6 Angle Controller

***Designer*: Mark Theng**

Inputs: none

Outputs: ANGLE, ABS, SIGN

2.6.1 Overview

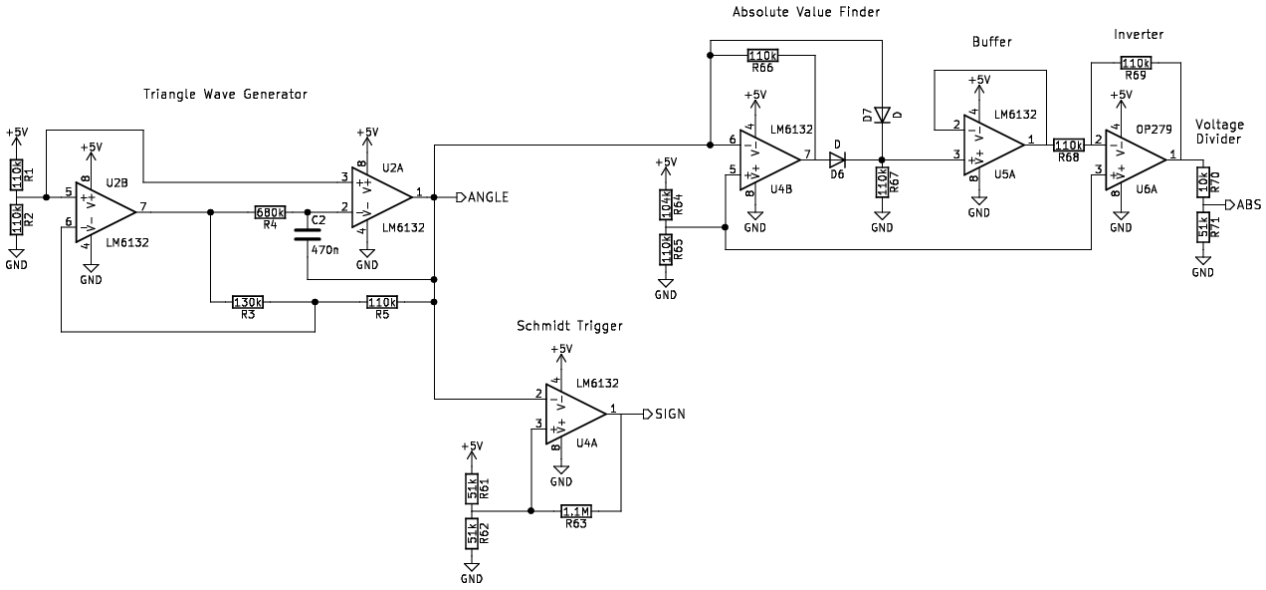

Figure 11: Angle Controller Module

A 1Hz triangle wave generator provides a periodic sweep on ANGLE for beamforming. The sweep from 0.5V to 4.5V represents a sweep between $-45°$ and $45°$. Since the beamforming module expects not the angle but the absolute value and sign of the angle, additional circuitry is used to compute these values, resulting in a 2Hz triangle wave from 0.5V to 2.5V for ABS and a 1Hz square wave for SIGN.

2.6.2 Circuit Insights

We generate the triangle wave by integrating a square wave with an op amp integrator. Note that the requirements for this module is rather dissimilar from most triangle wave generators. We are not concerned with the frequency of the triangle wave as much as its minimum and maximum limits, since we want the beamforming angle to sweep throughout and only within the full $90°$ range. Thus, instead of independently generating a square wave for integration, we set up a feedback loop so that the triangle wave is itself thresholded to produce the square wave, ensuring that the triangle wave switches direction at predetermined minimum and maximum voltages. At the same time, this design choice avoids the extremely long set-up time that would result from an AC-coupled integrator, which is especially pertinent since the signal frequency is so low.

The sign of the triangle wave is taken using a Schmidt trigger. We do this instead of using a MOSFET thresholding circuit (like in the timer module) because we want to set the virtual ground precisely at 2.5V, which can be more easily configured by resistors than a Zener diode. A Schmidt trigger is used instead of direct thresholding because the extremely slow variation of the 1 Hz triangle wave means that there is ample opportunity for noise to cause large oscillations in a simple thresholding circuit.

The absolute value of the triangle wave (where zero is defined as 2.5V) is found by taking the maximum voltage of the triangle wave when raw and when passed through an op amp negator (as shown in Fig. 11). By putting a large resistor at the output of the diodes,

we ensure that the current flowing through the diodes is very low, minimizing crossover distortion. To keep this high output resistance, an op amp buffer is used to isolate the output from the diodes.

As configured, the absolute value circuit gives a voltage between 2.5V and 4.5V, but the beamforming module expects a voltage between 0.5V and 2.5V. Thus, the output of the absolute value circuit is fed into an inverter. A voltage divider was later added to empirically correct for errors introduced by resistor tolerances.

Note that the absolute value circuit could have instead been designed to give voltages within the 0.5V to 2.5V range directly by reversing the directions of the diodes, obviating the need for the extra inverter. We chose to use the extra inverter because this leaves the "positive" output of the absolute value available. Future extensions of this project can use the "positive" absolute value to display readings in Cartesian rather than polar coordinates, which would be more intuitive for the viewer.

2.7 Timer

***Designer*: Mark Theng**

Inputs: none

Outputs: TICK (1ms 5V trigger every 6ms), OUT (0V – 4.5V)

2.7.1 Overview

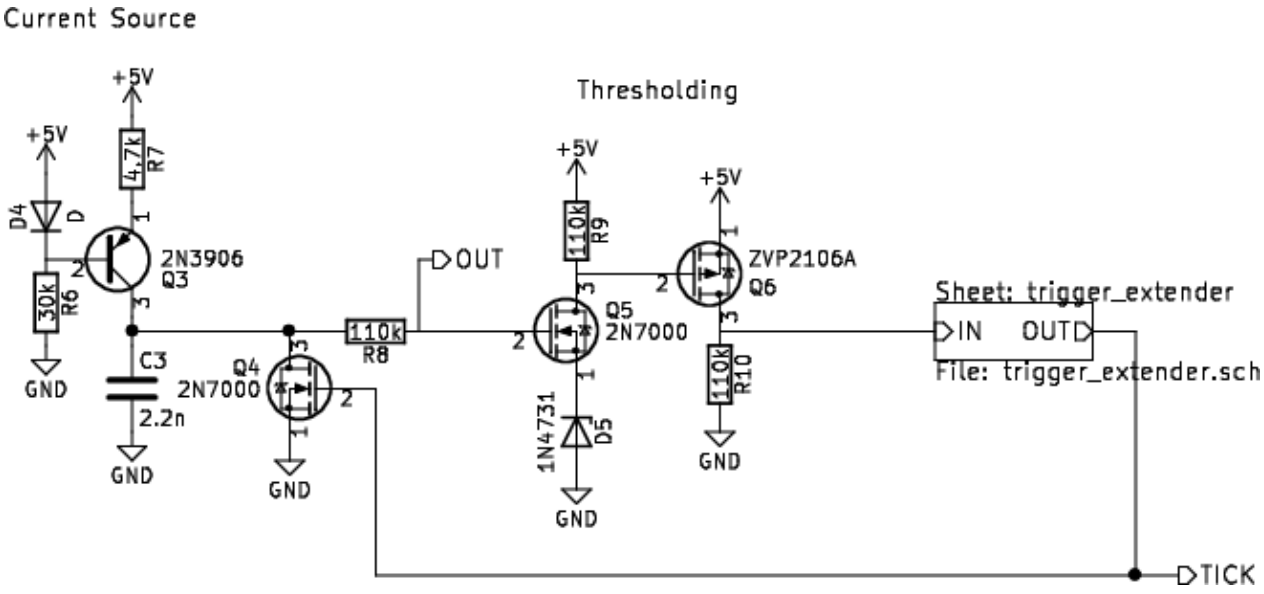

Figure 12: Timer Module

The distance of an object from speaker and microphones is determined by measuring the amount of time taken for the pulse from the speaker to echo off the object and reach the microphone. To time this, we use a BJT constant current source feeding into a capacitor. The charge on the capacitor thus gives an indication of the amount of time that has passed.

The voltage across the capacitor, which is proportional to the charge in the capacitor, is tied to the OUT output. OUT would be sampled by the sampling circuit when the beamforming arrays detects a returning audio pulse to provide the distance measurement.

When the charge on the capacitor reaches a given threshold, a pulse is sent on the TICK output, which would be converted into an audio pulse by the sound circuit. At the same time, a MOSFET is used to reset the timer by emptying the charge on the capacitor. The resulting output on OUT resembles a sawtooth wave with a period of roughly 6ms.

2.7.2 Circuit Insights

The BJT current source is adapted from the eCircuitCenter's topology[1]. The voltage across the emitter resistor is fixed by the difference between the diodes' turn-on voltages and the BJT's base-emitter voltage, resulting in a constant current flowing into the capacitor.

In our case, since the 1N914's turn-on voltage is larger than the 2N3906's base-emitter voltage, only one diode was necessary for the BJT current source. Using only one diode allowed us to increase the range of the timer, since the maximum voltage of the capacitor is limited by the voltage drop across the diodes.

The timing capacitor's value allows us to tweak the range and sensitivity of the timer. As the value of the capacitor is reduced, the voltage across the capacitor rises more quickly, increasing the timer's sensitivity but – since the timer is reset once it rises above a fixed threshold – decreasing the timer's range. Since the threshold is constrained to be less than the power supply voltage, there is a fundamental tradeoff between sensitivity and range. When we found that we were limited to much shorter distances than originally planned, we decreased the capacitor's value to its present value to improve the timer's sensitivity.

An important insight in this circuit is the resistor between the timer output and OUT (R8 in Fig. 12). While the timer circuit expects a very high load resistance on OUT, the nontrivial capacitance on OUT – such as the input capacitance of the op amp in the sampling circuit – caused pulses to propagate back into the timer capacitor, making the measurement unreliable. The resistor on OUT alleviates this by isolating the sensitive timer capacitor from the rest of the circuit.

A simple, MOSFET-base thresholding circuit is used to detect when the timer has reached its maximum value. Since the timer's value only increases during the thresholding period, a Schmidt trigger was not necessary, allowing us to reduce our circuit's complexity. In the thresholding circuit, the Zener diode provides the thresholding offset. When the input to the threshold rises above the sum of the MOSFET's turn-on voltage and the Zener voltage, the inverter's output would be brought low. Using a Zener diode in this topology allowed us to easily configure the threshold of the thresholding circuit, allowing the timer to use the full range of available voltages. An additional PMOS inverter stage improves the nonlinearity of the thresholding circuit's output.

A pulse extender (Fig. 13) is used to ensure that the charge on the timer capacitor is cleared completely during a reset. Without the pulse extender, direct feedback from the thresholding circuit to the reset MOSFET would cause the reset signal to drop once the capacitor voltage falls below the threshold. This would prevent the capacitor charge from being reset completely, and the circuit would instead stabilize into a steady state.

The pulse extender alleviates this by extending trigger pulses received at its input. When its input goes high, its capacitor is reset to 5V. After that, even if its input drops, the voltage across the capacitor would remain high for a predetermined period of time, since the capacitor would discharge slowly through the resistor. This allows the output of the trigger extended

[1] http://www.ecircuitcenter.com/Circuits_Audio_Amp/BJT%20Current_Source/BJT_Current_Source.htm

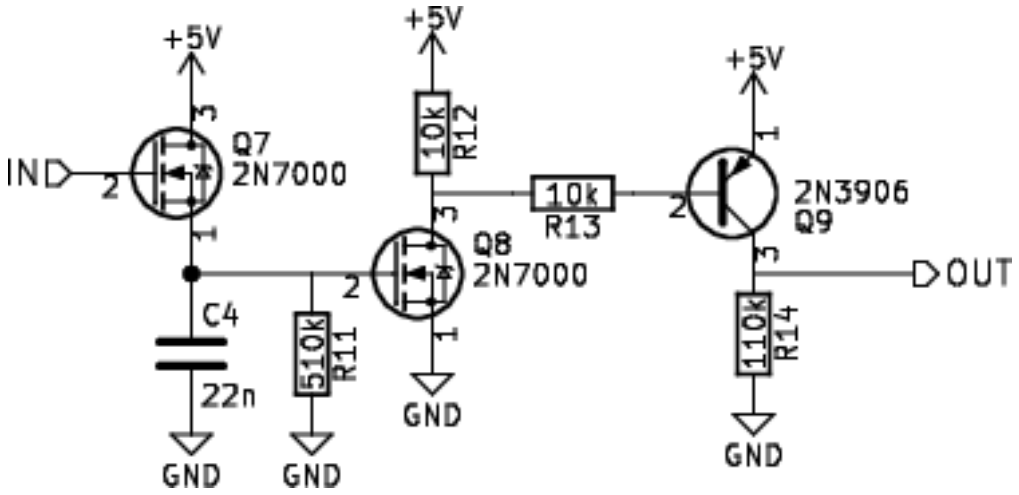

Figure 13: Pulse Extender used in the timer module

to remain high for a long enough period of time to fully reset the timer capacitor, even if the thresholding circuit's output subsequently falls.

An important detail is the BJT buffer. It provides a relatively low output resistance, isolating the pulse extender circuit from the output and keeping the output close to 5V during the entire extent of a pulse. The resistor on the base of the BJT was necessary to prevent what would effectively have been a short circuit from the BJT's emitter through the MOSFET to ground during the extent of a pulse.

2.8 Sampler

***Designer*: Mark Theng**
Inputs: IN (0V – 4.5V), TRIGGER (>100us >4.5V trigger)
Outputs: NOTIFY (1ms 5V trigger), OUT (0V – 4V)

2.8.1 Overview

When the return signal is received by the microphones, the signal conditioning module would transmit a short trigger pulse to the sampler via TRIGGER. This enacts a series of trigger delays, resulting a sequence of three actions:

1. The sample-and-hold circuit is reset.
2. The timer (via IN) is sampled into the sample-and-hold circuit.
3. If the time (and thus the distance to the detected object) is sufficiently small, a pulse is sent on NOTIFY so that the object's coordinates would be drawn on the screen.

The sampled time is also made available to the drawing module via OUT.

2.8.2 Circuit Insights

Since the length of the TRIGGER pulse depends on the precise parameters of signal conditioning, a pulse limiter is used to normalize the length of input pulses. It works similar to

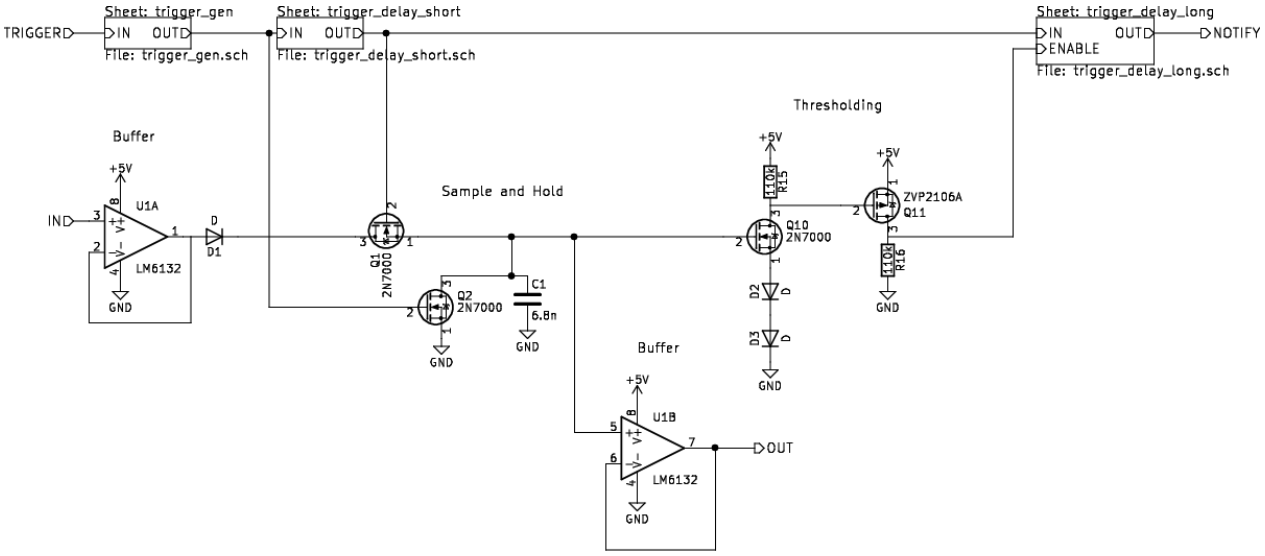

Figure 14: Sampler Module

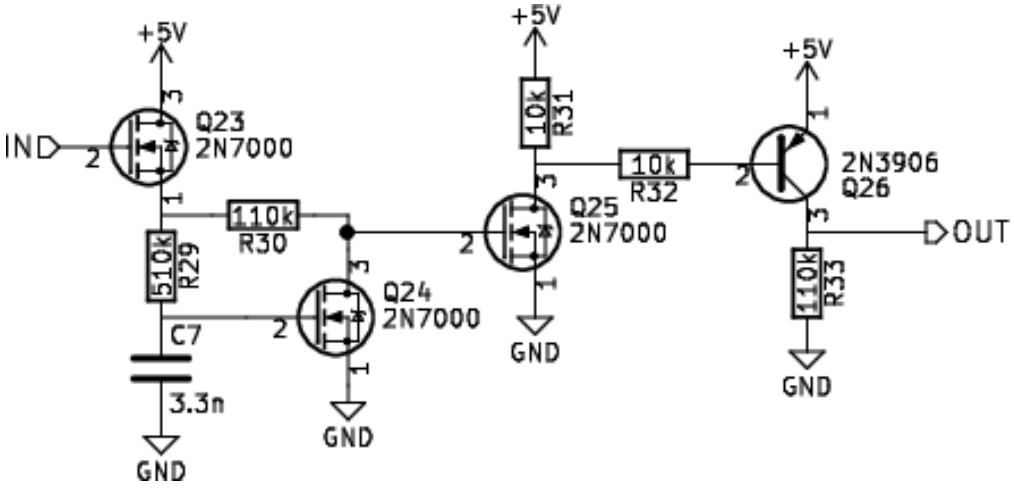

Figure 15: Pulse limiter used in the sampler module.

the pulse extender in the timer circuit. If the input is held high for a sufficiently long period of time, the capacitor would fill, turning on the MOSFET and causing the inverter's input to drop.

The "textbook" topology for a sample-and-hold circuit involves a transistor controlling an op amp buffer feeding into a capacitor, such as the one presented in Electronics Coach[2]. When the transistor is turned on, the voltage from the buffer is sampled onto the capacitor. After the transistor is turned off, the voltage on the capacitor is held constant even if the input to the op amp changes.

This topology, however, was not sufficient for our project. This is because real-life MOSFETs have a body diode, so it is necessary to ensure that (for an NMOS) the drain voltage is always higher than the source voltage. This would not be the case, for example, if the input voltage decreases after being sampled, which could happen when the timer is reset.

In real sample-and-hold circuits, this problem is usually circumvented by using a JFET

[2] https://electronicscoach.com/sample-and-hold-circuit.html

instead of a MOSFET, since JFETs do not have a body diode. However, the available JFETs required a very low turn-off voltage, which was not feasible for our low power supply voltages.

To alleviate this, the diode just after the op amp buffer ensures that current can only flow in one direction through the MOSFET. The turn-on voltage of the diode causes the voltage saved onto the capacitor during sampling to be about 0.5V less than the voltage received on IN. This does not affect circuit correctness since the error is systematic and thus contributes only to a constant offset subtracted from the measured voltages.

Using a diode in this manner requires that the voltage on the capacitor must always be lower than the voltage on IN just before sampling. This is achieved by the first stage in the three-stage sequence, where a MOSFET brings the sampling capacitor's voltage down to zero.

Due to the high sensitivity of the sampling capacitor, the sampled voltage is passed through an op amp buffer before being presented on OUT.

The thresholding circuit is similar to the one used in the timer module. However, due to the very low voltages involved, there were no Zener diodes with a small enough Zener voltage to provide the necessary threshold. Thus, two diodes are used instead.

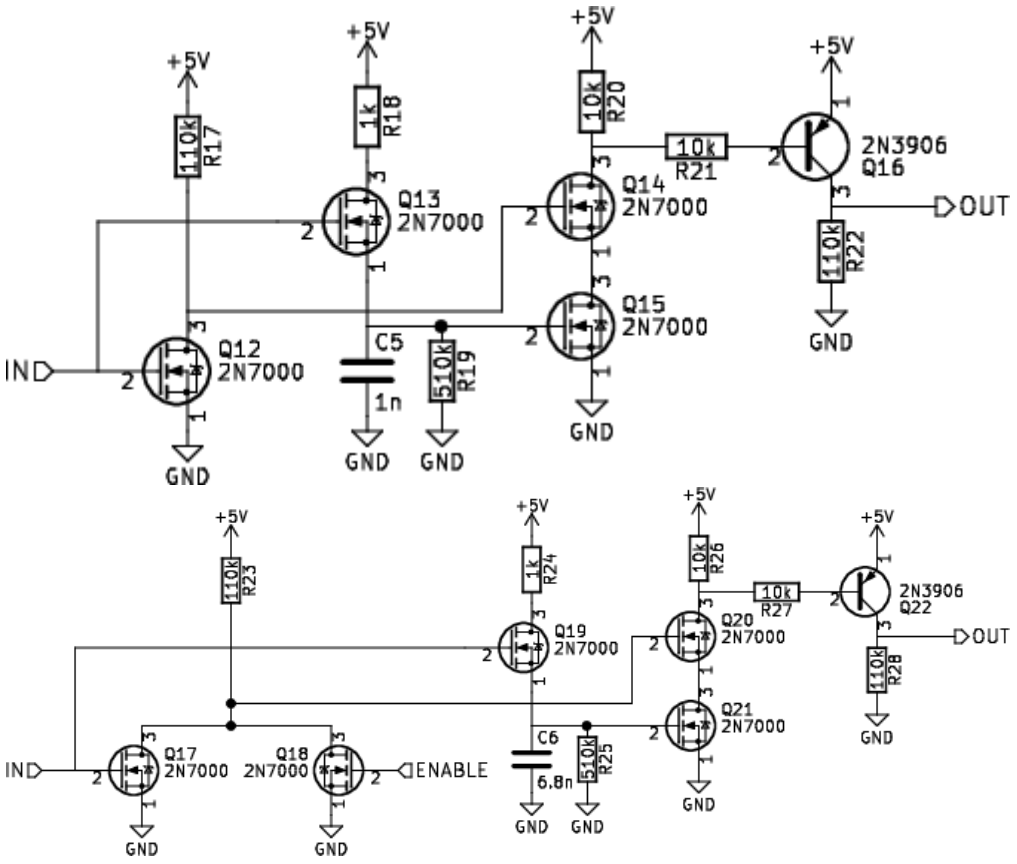

Figure 16: Trigger delay circuits used in the sampler module. Top: First (short) trigger delay. Bottom: Second (long) trigger delay.

The trigger delay is similar to the pulse extender circuit used in the timer module. Rather than actually delaying the input trigger, this trigger delay submodule fakes a delay by generating a new trigger on the falling edge of the input trigger. This allows the output trigger to be of a different length from the input trigger, which allowed us to independently control

the length of NOTIFY, the drawing pulse.

2.9 Drawing

***Designer*: Mark Theng**
Inputs: ANGLE (0.5V – 4.5V), DIST (0V – 4V), ENABLE (1ms >4.5V trigger)
Outputs: Circles drawn on the oscilloscope

2.9.1 Overview

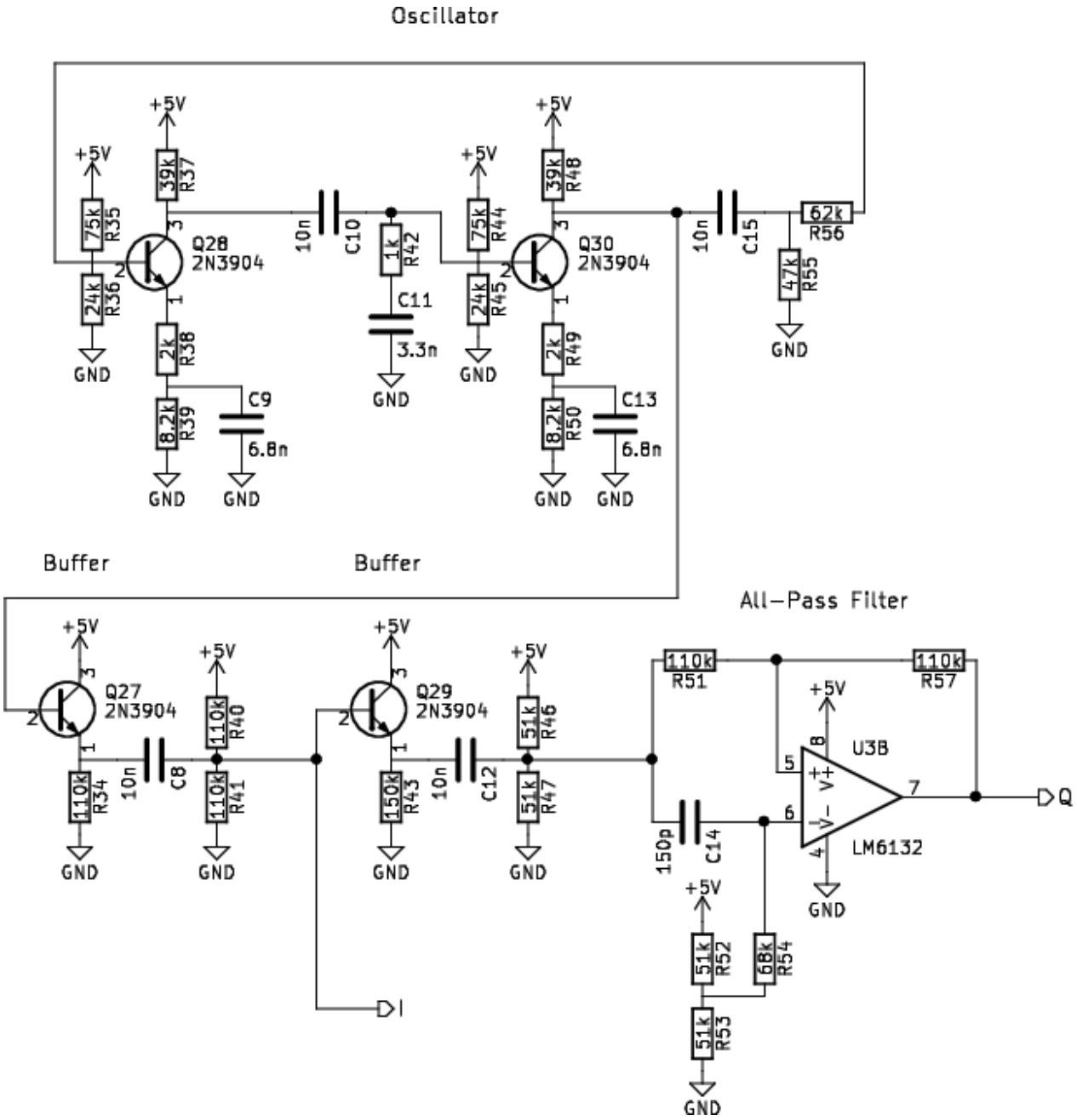

Figure 17: Circle drawing submodule of the drawing module.

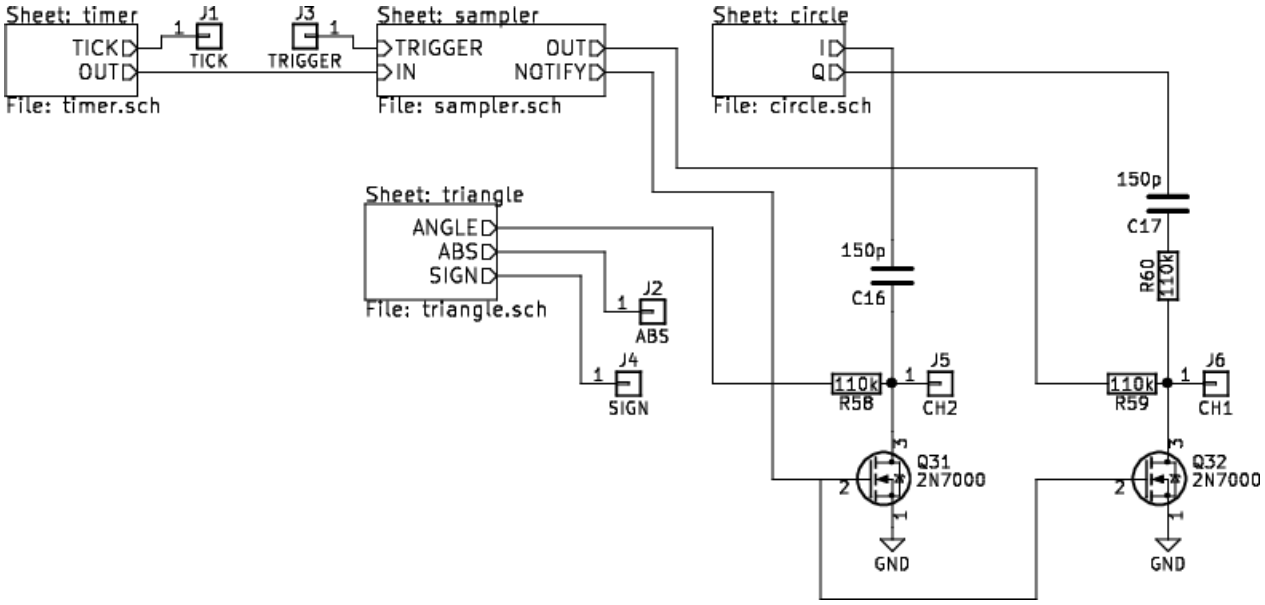

Figure 18: Summing the oscillator outputs with the angle and distance readings in the drawing module.

An oscillator with internal band-pass filtering produces a clean sine wave at roughly 15kHz. This is passed into an all-pass filter, which shifts the phase of the signal by 90°. This, along with the raw oscillator output, provides the in-phase and quadrature signals that, when added to ANGLE and DIST respectively, provide the x- and y- coordinates for drawing circles indicating the positions of detected objects on the oscilloscope. ENABLE enables drawing only when a reading is obtained from the microphones.

2.9.2 Circuit Insights

The oscillator is made by connecting two band-pass inverting BJT amplifiers into each other. This is used instead of an RC phase-shift oscillator since it provides a larger signal amplitude for a lower power consumption. Additionally, the internal band-pass filters obviate the need for band-pass filters on the output, since the sine wave produced by the oscillator is already clean.

Even then, the amplitude of the signal produced by the oscillator is small, since the low supply voltage requires us to limit the amplitude of the signal to prevent the signal from being distorted by the BJTs. The amplitude of the signal can be adjusted by tweaking the 47k resistor (R55 in Fig. 17) near the point where the output is taken from the oscillator.

Since the amplitude of the oscillator signal is already so small, we can't afford to lose more amplitude when passively adding the signal to ANGLE, or when feeding it into the all-pass filter. BJT buffers are thus used to isolate the oscillator from the rest of the drawing circuit.

3 Building Process

Due to the repetitive nature of the beamforming circuit, we initially wanted to build it directly on a surface-mounted PCB. However, despite designing and submitting the PCB early, we

faced severe delays in ordering the PCB, requiring us to give up on the PCB altogether. In the resulting shortage of time, we opted to implement just three microphones for the beamforming array instead of the original seven planned. Since the number of voltage-controlled phase shifters increased quadratically with the number of microphones, this drastically reduced the amount of last-minute breadboarding necessary to complete the project.

Since the distance between the microphones was important, and since the microphone module was the most sensitive, we opted to solder the microphone amplifier circuits onto a protoboard.

Using only three microphones made the implementation of the circuit more challenging since the signal we received was of very low quality. Specifically, as seen in Figure 7, the amplification lobes for beamforming were a lot wider, resulting in a poor angle resolution. Furthermore, the attenuation for signals coming from directions other than the direction of beamforming was significantly lower, resulting in a much lower signal-to-noise ratio.

Another difficulty we faced was that the speaker that we ordered was not loud enough to get reliable echoes over a large distance. To alleviate this, we swapped it out for a significantly louder lab speaker. However, the lab speaker was not omnidirectional, adding further difficulties to the angle measurement. Even then, it was necessary to use a hard, flat surface, held at just the right angle, to produce a return signal loud enough for us to distinguish from the ambient noise.

As a result, signal conditioning proved to be the most challenging part of our project. At one point, we were receiving short, periodic pulses from the microphones' output, and were unable to determine their cause. We eventually resolved it by adding a low-pass capacitor and an additional inverting amplifier stage. However, the inversion required substantial changes to the signal conditioning circuit to correctly detect signal amplitudes.

Power supply coupling also proved to be a significant issue. The speaker drew a lot of power, resulting in a large amount of power supply noise that would get amplified by the microphone amplification stages. The simplest solution was to use a separate power source for the speaker module.

Even then, since we were sending pulses from the timer circuit to the speaker, we still had to connect the ground of the speaker module to the rest of the circuit. The small amount of noise that the speaker caused in ground still resulted in a significant amount of noise after amplification through the microphones' multiple stages. We eventually resolved that by connecting the microphone's and speaker's ground on opposite ends of the control circuitry's breadboard, and adding large capacitors to the power supplies of both modules.

4 Conclusion

We designed and constructed a rudimentary rangefinding system with linear array beamforming system. Our final tests were mostly qualitative rather than quantitative, and we could clearly see that changes in distance provided the anticipated changes. While our three microphone system only provides a proof of concept, we completed a PCB design intended for a larger system that could potentially be used as a starting point for a larger digital project in a future year. Another student could easily pick up the microphone array design, add ADCs to each output, and attempt to do more sophisticated wideband processing digitally.

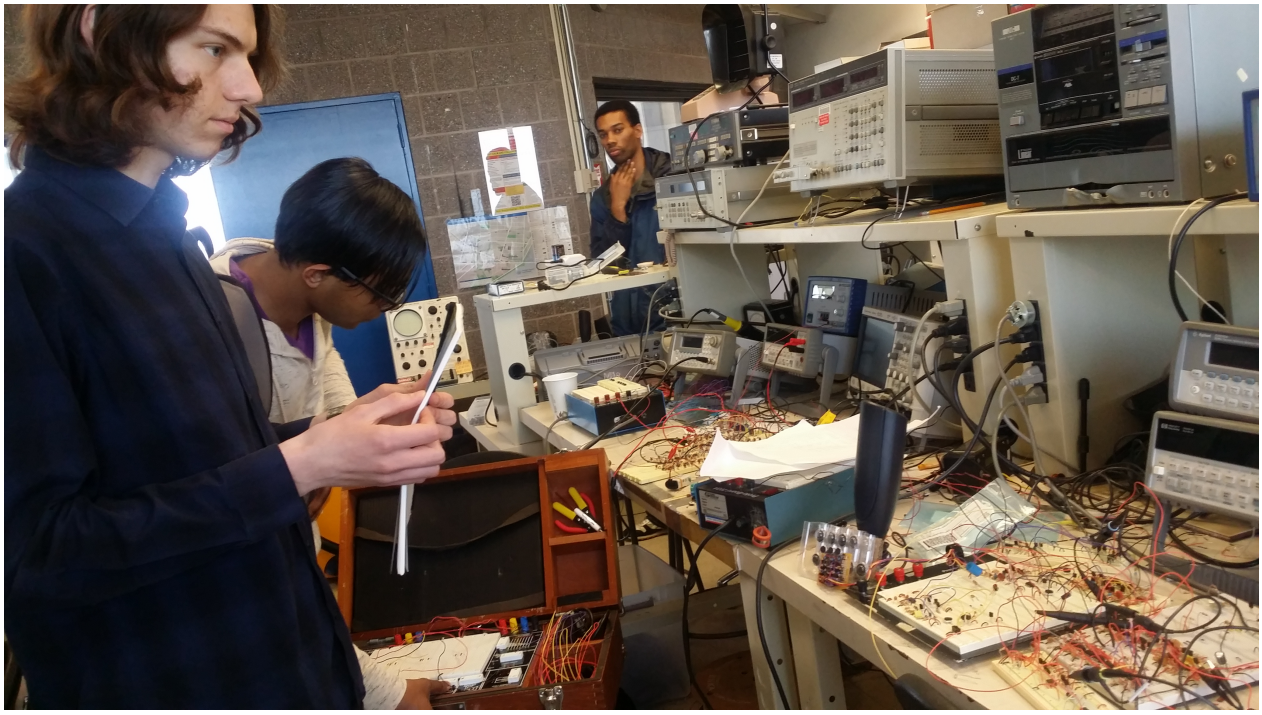

Figure 19: Left: Flat surface used to reflect the sound pulse from the speaker to the microphones. Right: Physical setup of the speaker and microphones.

References

[1] D. Pantzartzis, D. Alexandrou, and V. Premus, "High-resolution bathymetric simulations based on kirchhoff scattering theory and anisotropic seafloor modeling," in *Acoustics, Speech, and Signal Processing, 1994. ICASSP-94., 1994 IEEE International Conference on*, vol. ii, Apr 1994, pp. II/353–II/356 vol.2.

[2] B. Wang, Q. Xu, C. Chen, F. Zhang, and K. J. R. Liu, "The promise of radio analytics: A future paradigm of wireless positioning, tracking, and sensing," *IEEE Signal Processing Magazine*, vol. 35, no. 3, pp. 59–80, May 2018.

[3] P. Horowitz and W. Hill, *The Art of Electronics*. Cambridge University Press, 2015.

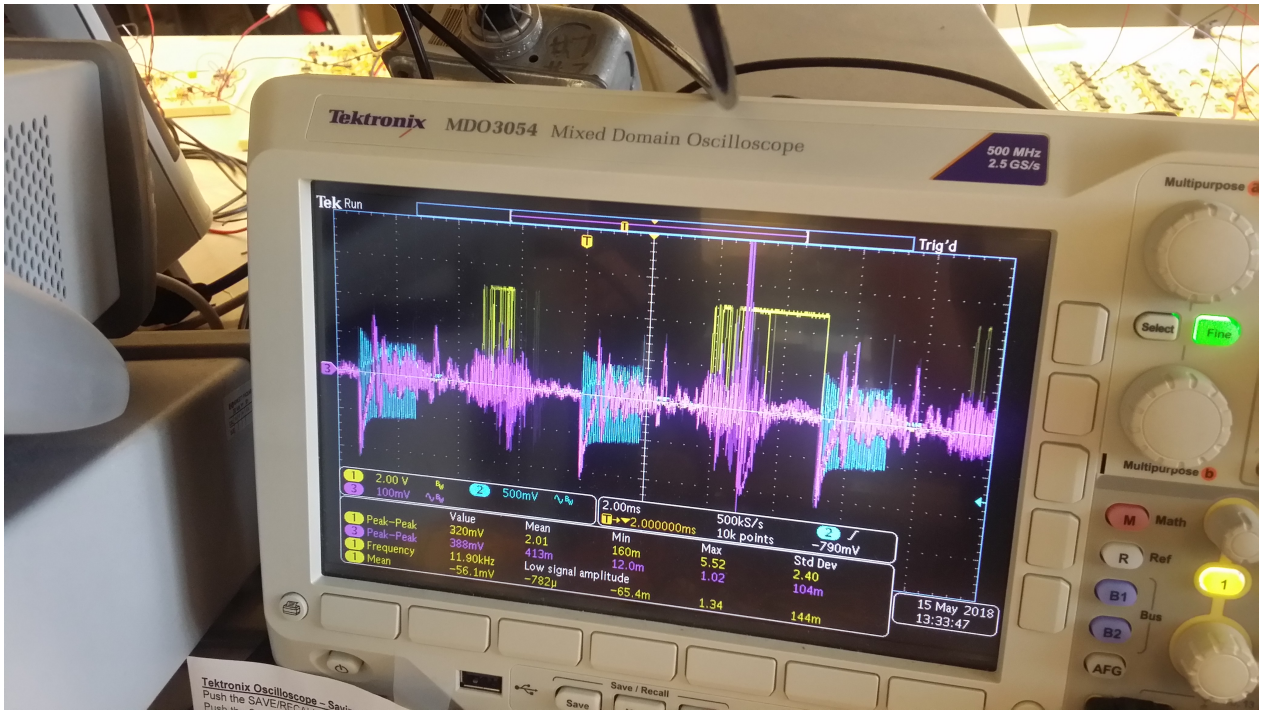

Figure 20: Blue: Microphone output. Purple: Signals detected by the microphones after beamforming. Yellow: Pulses emitted by signal conditioning. Note that there is a visible echo in the purple trace shortly after a sound pulse is emitted.

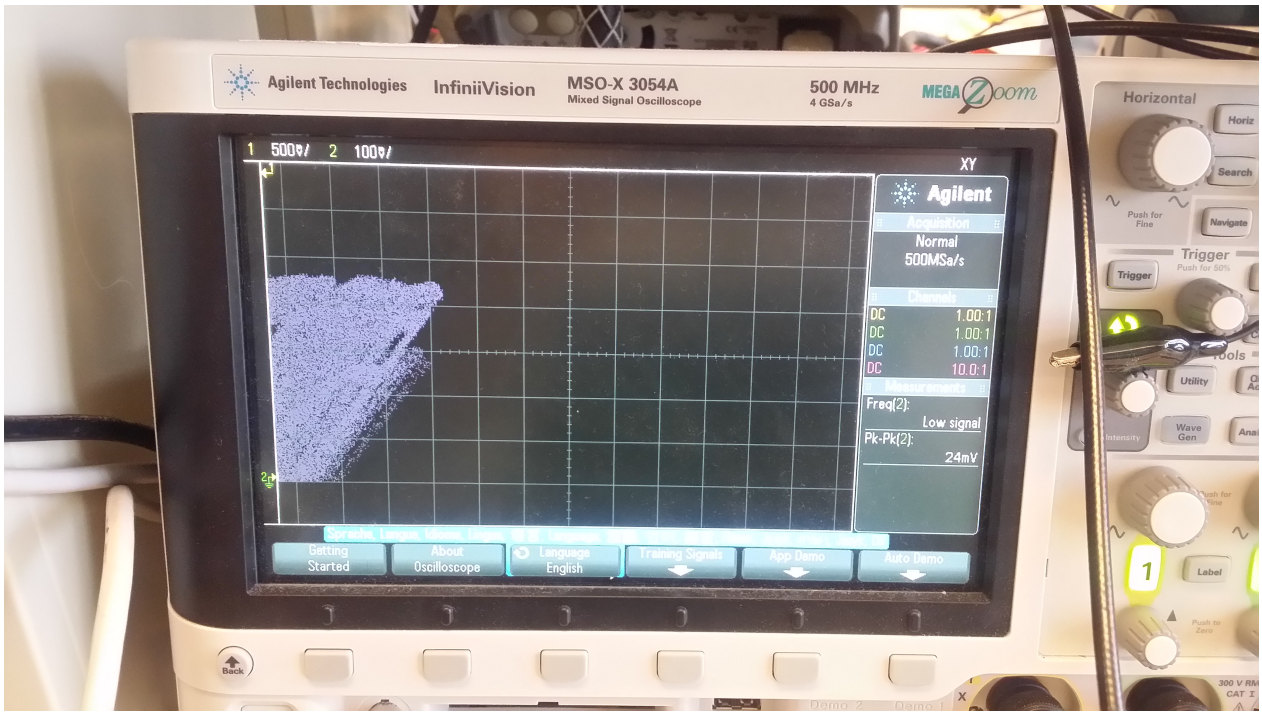

Figure 21: Final XY output. While the output is not very clear in this sample due to the low precision of the signal, we see that most of the readings are drawn in the upper half of the oscilloscope, indicating that the barrier is somewhere to the left of the setup.